Editors' Suggestion

Probing Quantum Phases in Ultra-High-Mobility Two-Dimensional Electron Systems Using Surface Acoustic Waves

Mengmeng Wu,[1] Xiao Liu,[1] Renfei Wang,[1] Yoon Jang Chung,[2] Adbhut Gupta,[2] Kirk W. Baldwin,[2] Loren Pfeiffer,[2] Xi Lin,[1,3,*] and Yang Liu[1,†]

[1]*International Center for Quantum Materials, Peking University, Haidian, Beijing 100871, China*
[2]*Department of Electrical Engineering, Princeton University, Princeton, New Jersey 08544, USA*
[3]*Interdisciplinary Institute of Light-Element Quantum Materials and Research Center for Light-Element Advanced Materials, Peking University, Haidian, Beijing 100871, China*

(Received 5 July 2023; revised 21 November 2023; accepted 16 January 2024; published 12 February 2024)

Transport measurement, which applies an electric field and studies the migration of charged particles, i.e., the current, is the most widely used technique in condensed matter studies. It is generally assumed that the quantum phase remains unchanged when it hosts a sufficiently small probing current, which is, surprisingly, rarely examined experimentally. In this Letter, we study the ultra-high-mobility two-dimensional electron system using a propagating surface acoustic wave, whose traveling speed is affected by the electrons' compressibility. The acoustic power used in our Letter is several orders of magnitude lower than previous reports, and its induced perturbation to the system is smaller than the transport current. Therefore we are able to observe the quantum phases become more incompressible when hosting a perturbative current.

DOI: 10.1103/PhysRevLett.132.076501

Two-dimensional electron systems (2DES) with extremely low disorder host a plethora of exotic quantum many-body states [1–3]. The quantum Hall state (QHS) is incompressible signaled by vanishing longitudinal resistance and quantized Hall resistance [3]. At high Landau level fillings factors $\nu > 4$, various charge density waves are stabilized by the large extent of the electron wave function [4–6]. The enigmatic 5/2 fractional quantum Hall state (FQHS) attracts tremendous interest [7–16] because its quasiparticles might obey non-Abelian statistics [17–20]. Various experimental studies have studied its topological properties and quasiparticle statistics, such as weak tunneling [21–24], interferometry [25–28], shot noise [29–32], and thermal transport [33–35]. Most of these studies rely upon the hypothesis that a quantum state is unperturbed by the tiny probing current passing through the μm size device.

Surface acoustic wave (SAW) is a useful current-free technique to investigate the property of 2DES [36–44]. The propagating piezoelectric field accompanying the SAW interacts with the charge carriers, which in turn affects its velocity (v) and attenuation. Qualitatively, this interaction is related to the compressibility of 2DES: v increases when the 2DES becomes incompressible and thus unable to respond to the SAW [45]. In this Letter, we probe the 2DES using a pW-level, continuous-wave SAW and discover that the ~100 nA current flowing through the ~1 mm size sample causes a ~0.1 ppm (parts per million, 10^{-6}) increase of the SAW velocity at very low $T \lesssim 250$ mK. Such a current-induced SAW velocity shift illustrates that a close and careful examination on the charge transport mechanism is essential and imperative.

Our sample is made from a GaAs/AlGaAs wafer grown by molecular beam epitaxy. The 2DES is confined in a 30-nm-wide quantum well, whose electron density is 2.91×10^{11} cm^{-2} and low-temperature mobility is about

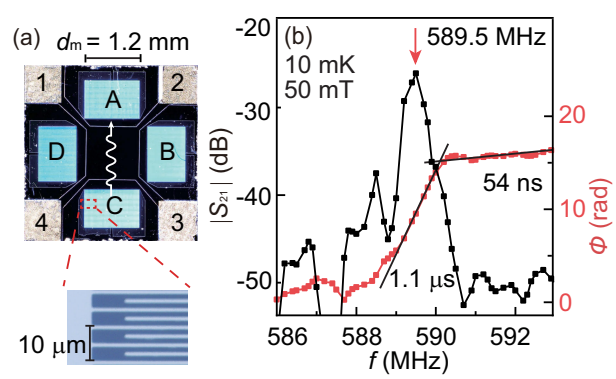

FIG. 1. (a) Photo of our device. The enlarged plot shows the structure of the aluminum IDT. Two pairs of orthometric IDTs are evaporated on the sample labeled by the letters A to D, and four contacts are made at the four corners labeled by numbers 1 to 4. IDT C is used to excite the SAW and IDT A is used for receiving SAW. Unless otherwise specified, the current is injected into contact 1 and flows out from contact 2, while contacts 3 and 4 are floats. (b) The measured amplitude ($|S_{21}|$) and phase delay (Φ) of the transmission coefficient as a function of frequency at base temperature T and magnetic field $B \sim 50$ mT.

 © 2024 American Physical Society

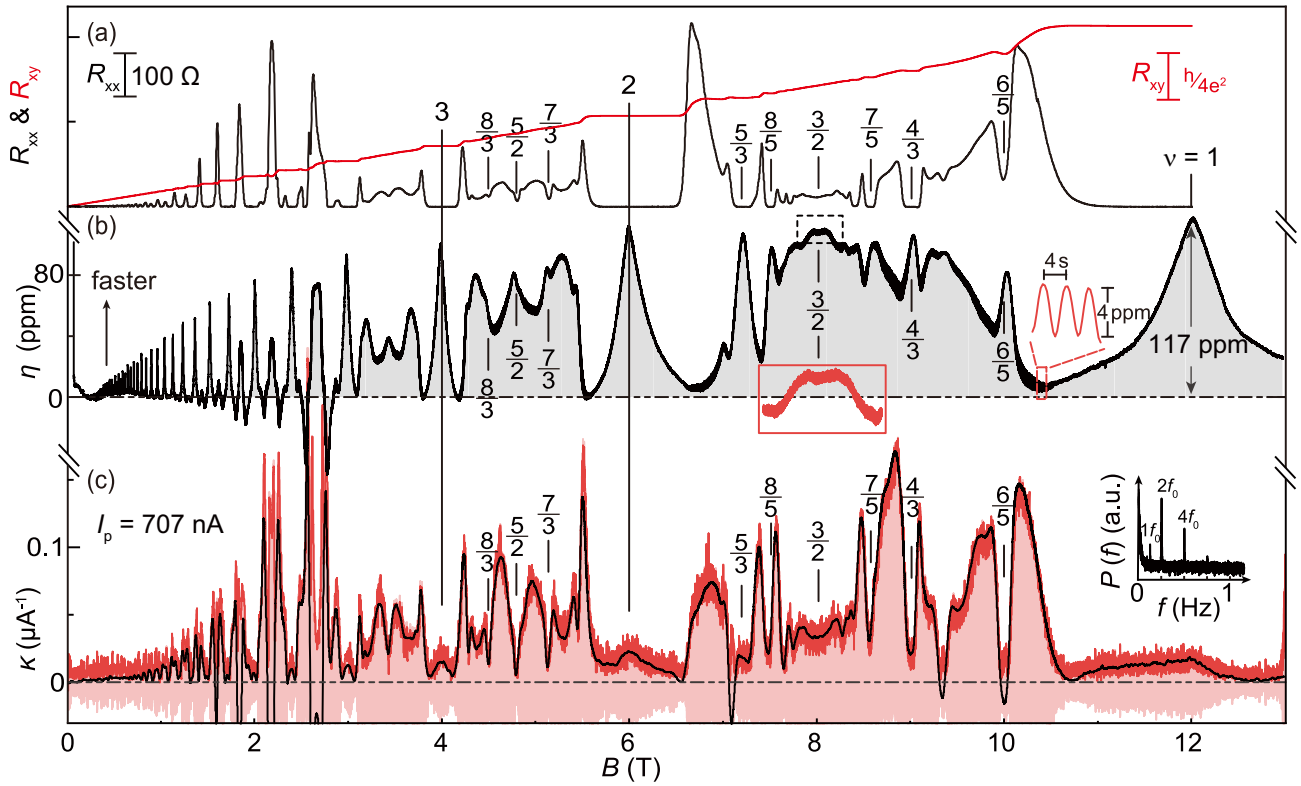

FIG. 2. (a) The longitudinal (R_{xx}) and Hall (R_{xy}) resistance vs B. (b) The measured SAW velocity increase $\eta(B) = \Delta v(B)/v_0$. A $f_0 = 0.125$ Hz, $I_p = 707$ nA ac current passes through the sample (contact $1 \to 2$) during the measurement, imposing a 4-s-period oscillation to η; see the enlarged plot in the red dashed box. Red solid box shows η near $\nu = 3/2$. (c) The extracted oscillation using a digital bandpass filter centered at 0.25 Hz (pink curve). Its amplitude can be measured using a lock-in amplifier (black curve). Inset: power spectrum density of the oscillation. The Y coordinate κ is defined as $\eta_m^{-1} \cdot (\partial\eta/\partial|I|)$. The meaning of κ is explained in Fig. 3.

2×10^7 cm^2/(V · s). We make a Van der Pauw mesa (length of side $d_m = 1.2$ mm) by wet etching, and then evaporate 5-μm-period interdigital transducers (IDTs) on each side of the mesa. A 50 Ω resistance is connected in parallel to each IDT for broadband impedance matching. When applied with an ac voltage whose frequency matches the resonance condition, the IDT generates a propagating SAW. The SAW will be captured by the IDT on the opposite side of the sample as a voltage output through the piezoelectric effect [46]; see Fig. 1(a).

We use a custom-built superheterodyne demodulation system [47] to analyze the attenuation $|S_{21}|$ and phase delay Φ of the output signal [48]. From the measured $|S_{21}|$ and Φ vs frequency f shown in Fig. 1(b), we can calculate the reference SAW velocity v_0 at low field ($\simeq$2950 m/s) from the IDT period (5 μm) and the resonant frequency f_c (589.5 MHz). We can also derive the delay time $\partial\Phi/\partial(2\pi f) = 1.1$ μs and 54 ns near and away from the SAW resonance peak, consistent with the ~3 mm SAW travel distance and ~11-m-long coaxial cable (5.5 m each way). The experiment is carried out in a dilution refrigerator whose base temperature is $\lesssim$10 mK.

Figures 2(a) and 2(b) show the magnetoresistance (R_{xx}, R_{xy}) and the measured relative SAW velocity increase $\eta(B) = \Delta v(B)/v_0$, where $\Delta v(B) = v(B) - v_0$. The positive (negative) velocity shift results in the decrease (increase) in the delay time. We can directly deduce η from the measured SAW phase shift Φ through $\eta \simeq -\Delta\tau/\tau = -\Phi/(2\pi f_c \tau)$, where $\tau = d_m/v_0 = 407$ ns is the SAW's traveling time through the 2DES. At high B fields, η exhibits maxima (corresponding to enhanced SAW velocity) when the 2DES forms an incompressible quantum Hall state and its screening capability vanishes [43]; see Fig. 2(b). The SAW interacts with 2DES by inducing a screening charge distribution. Therefore η is related to the 2DES compressibility $(dn/d\mu)$ [48]. η at integer fillings increases monotonically with decreasing ν. We linearly fit the data at $\nu \lesssim 10$ and define the intercept at $\nu = 0$ as $\eta_m = 124$ ppm [48].

Unlike the vanishing plateaus seen in R_{xx}, we observe "V"-shaped maxima in η. At the vicinity of integer filling factors $\nu = N + \nu^*$, N is an integer, the 2DES consists of an incompressible quantum Hall liquid and additional quasiparticles or quasiholes whose filling factor $|\nu^*| < 1$. The fact that η has a linear dependence on the quasiparticle or quasihole density $n^* = n|\nu^*|/\nu$ suggests that the quantum phase formed by these dilute quasiparticles or quasiholes is compressible [48,51]. The SAW velocity enhancement is

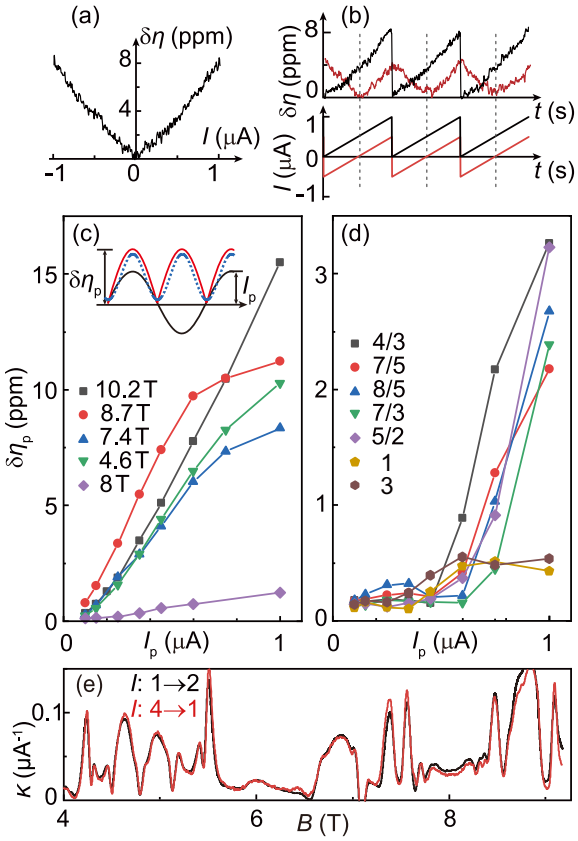

FIG. 3. (a) $\delta\eta$ vs dc current I at $B = 4.62$ T. (b) $\delta\eta$ vs time measured with different ranges of sweeping current (black and red). (c),(d) $\delta\eta_p$ vs current peak I_p at transition states and QHSs. Inset: black curve is the sinusoidal input current with peak amplitude I_p and frequency f_0. Red curve is the current induced velocity shift ($\delta\eta$) with amplitude $\delta\eta_p$. Blue dashed curve is the second harmonic component of $\delta\eta$. (e) κ vs B when current ($I_p = 707$ nA) flows perpendicular (between contacts 1 and 2) and parallel (4 and 1) to the SAW propagation direction.

also seen as clear "V"-shaped maxima at $\nu = 4/3$, $5/3$, $6/5$, etc., as well as developing maxima at $\nu = 5/2$, $7/3$, and $11/5$ where FQHSs develop. The SAW velocity enhancement is seen when the SAW propagates along the hard axis of the stripe phase formed at $\nu = 9/2$, $11/2$, etc., consistent with previous reports [42]. Interestingly, η is large near $\nu = 3/2$ where the 2DES forms compressible composite fermion Fermi sea, possibly because the composite fermions with extremely large effective mass are inert to the SAW-induced field [52].

We are able to reach ~0.1 ppm resolution in η while using excitation that is orders of magnitude smaller than previous reports [42]. The input excitation power in Fig. 2(b) is 1 nW (-61 dBmW) and only a tenth of it turns into SAW considering the attenuation of cables and the efficiency of the IDT. The SAW-induced potential on the 2DES is only ~10 μeV, leading to $\lesssim 10^4$ cm^{-2} electron density fluctuation [48]. Therefore, we can resolve very delicate response of 2DES while preserving the fragile many-body states. One of the most surprising discoveries is a velocity shift $\delta\eta = \eta(B, I) - \eta(B, I = 0)$ induced by a current passing through the 2DES; see Fig. 3(a). $\delta\eta$ increases nearly linearly by 8 ppm when I increases from 0 to 1 μA. $\delta\eta$ is an even function of I, so that if we sweep the current from −0.5 to 0.5 μA, η displays a triangle waveform; see Fig. 3(b). We define a parameter $\kappa = \eta_m^{-1} \cdot (\partial\eta/\partial|I|)$ to describe this current induced velocity shift (CIVS) effect.

We note if the input current is sinusoidal at frequency f_0, the leading component of $\delta\eta$ would be the second harmonic at frequency $2f_0$; see the Fig. 3(c) inset. Therefore, we can use lock-in technique to measure amplitude ($\delta\eta_p$) of the $\delta\eta$ oscillation from its second harmonic [48] and deduce $\kappa \simeq \eta_m^{-1} \cdot (\delta\eta_p/\delta I_p)$ even when the CIVS effect is small. We measure $\delta\eta_p$ at different filling factors as a function of the ac current amplitude I_p in Figs. 3(c) and 3(d). In the left panel where the 2DES is compressible, $\delta\eta_p$ increases linearly and then saturates at large current amplitudes. In the right panel, the tiny $\delta\eta_p$ value does not rise obviously with the increase of current at integer fillings. At fractional fillings, we discover a clear threshold behavior where $\delta\eta_p$ remains almost zero until I_p reaches about 600 nA.

The Fig. 2(b) data is taken when a $f_0 = 0.125$ Hz, $I_p = 707$ nA current passes through the 2DES. In the expanded plot of η in Fig. 2(b) and the power spectrum of the η in Fig. 2(c), we can clearly observe a 4-s ($2f_0$) period oscillation in η. We apply a digital band-pass filter to the Fig. 2(b) data to extract this oscillation (pink shade) and deduce κ from its amplitude (red trace) in Fig. 2(c). Alternatively, we can use a lock-in amplifier to measure this oscillation amplitude (black trace). The Fig. 2(c) data clearly evidence the dependance of CIVS effect on the quantum phases of 2DES. At strong quantum Hall effects, unlike the "V"-shaped maxima in the η trace and the plateau in the R_{xx} trace, κ presents a "W"-shaped minimum—it has a positive peak at exact integer $\nu = 1, 2, 3$, etc. and reduces to zero on both sides before increasing. Between $\nu = 1$ and 2, κ exhibits clear minima at $\nu = 4/3$, $5/3$, $7/5$, $8/5$, and $6/5$ when FQHSs form, similar to the η and R_{xx} traces. Surprisingly, a clear minimum can be seen in the κ trace corresponding to the fragile FQHS at $\nu = 5/2$, $7/3$, $8/3$, $11/5$, and $14/5$, while the η trace only shows a glimmer of maxima.

We can rule out the possibility that finite κ is caused by the heating effect. As discussed in the Supplemental Material [48], η has little temperature dependence when the sample temperature is below 100 mK. Although there is no reliable approach to detect the electron temperature of the 2DES, we are quite confident that it is well below 100 mK when taking Fig. 2 data. We can see clear features in η and κ in Figs. 2(b) and 2(c) for several fragile quantum phases such as the FQHSs at $\nu = 5/2$, $7/3$, and $8/3$ and the unidirectional charge density waves at $\nu = 9/2$ and $11/2$, which are only stable at temperatures well below 100 mK.

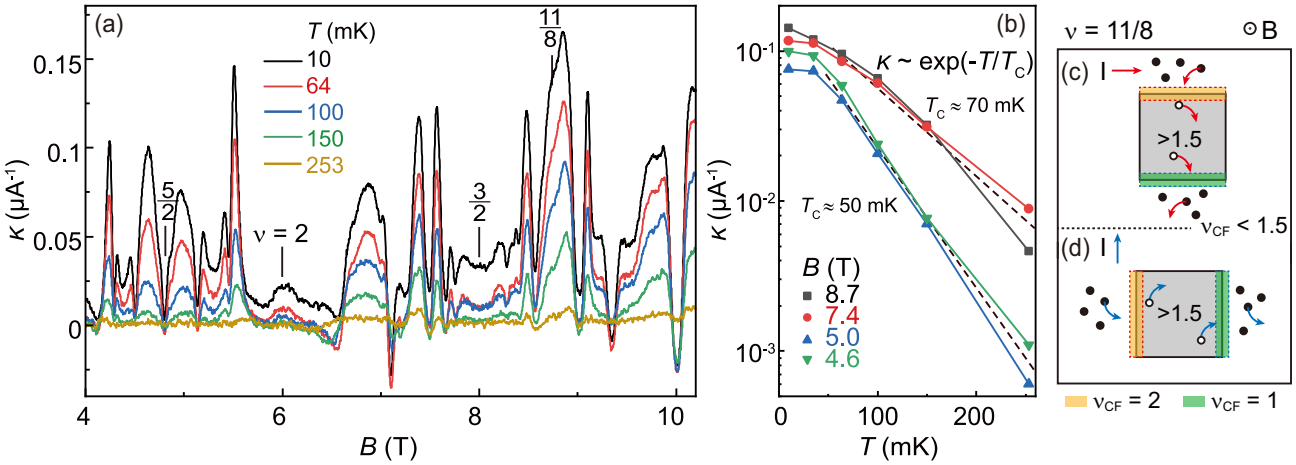

FIG. 4. (a) κ vs B at different T. (b) κ vs T at different B. (c),(d) Schematic explanation of the CIVS at $\nu = 11/8$. Solid and open dots represent negative-charged quasiparticles and positive-charged quasiholes respectively. (c) and (d) depict situations when currents flow on different directions. The dashed box represents the phase boundary. The gray (white) domain is the region with $\nu_{\mathrm{CF}} > 1.5$ ($\nu_{\mathrm{CF}} < 1.5$).

The transport measurement taken using 500 nA rms current also shows clear difference when temperature raises to 100 mK [48]. Lastly, κ dip at a fragile QHS such as $\nu = 5/2$ is much more obvious than the composite fermion Fermi sea at $\nu = 3/2$, although the former is more sensitive to the temperature.

Figure 4(a) shows that at all fields κ decreases as T increases, and eventually vanishes when $T \simeq 250$ mK. The summarized κ vs T data at different fields in Fig. 4(b) suggests an exponential dependence $\kappa \propto \exp(-T/T_{\mathrm{C}})$ where the characteristic temperature T_{C} is about 50 mK at $2 < \nu < 3$ and 70 mK at $1 < \nu < 2$. More data show that the T_{C} is insensitive to the probing SAW frequencies or wavelengths [48]. It is important to mention that the vanishing of κ is unlikely a direct result of reduced quantum Hall stability, since the QHS around 3/2 remains quite strong at $T \simeq 250$ mK when κ vanishes.

The measured κ is almost always positive. The increased SAW velocity suggests that the 2DES becomes more incompressible when carrying current. Intuitively, the current cripples the incompressible phases by introducing more defects or inhomogeneities and broadening the domain walls, so that the 2DES is are expected to be more compressible. Also, we observe no change in κ when we rotate the current direction to be parallel to SAW [see Fig. 3(e)], indicating that the CIVS has no dependence on which direction the current flows. Unfortunately, there is very little investigation on the morphing of the quantum phase when carrying a nondestructive current. Meanwhile, the large κ is seen at the transition between two neighboring QHSs, where a rigorous description of charge transport mechanism must involve quasiparticle localization and percolation, which is particularly hard.

We propose a simple hand-waving mechanism to understand the positive κ in Fig. 4(c). At $\nu = 4/3$ and 7/5, the electrons in the partially filled Landau level form $\nu = 1/3$ and 2/5 fractional quantum Hall states, respectively, if the 2DES is fully spin-polarized. These two states can be explained as the $\nu_{\mathrm{CF}} = 1$ and 2 integer quantum Hall states of composite fermions, and the phase transition happens at $\nu = 11/8$ when the average composite fermion filling factor $\langle \nu_{\mathrm{CF}} \rangle = 1.5$. Because of the density fluctuation [53], the regions with $\nu_{\mathrm{CF}} < 1.5$ ($\nu_{\mathrm{CF}} > 1.5$) consist of an incompressible $\nu = 4/3$ ($\nu = 7/5$) QHS and additional movable negative-charged quasiparticles (positive-charged quasiholes); see Fig. 4(c). When a current passes through the sample, e.g., from left to right (red arrow), quasiparticles move leftward and quasiholes move rightward. The effective magnetic field poses a Lorentz force, leading to the accumulation and depletion of quasiparticles or quasiholes at the phase boundary. The depletion (accumulation) of quasiholes and accumulation (depletion) of quasiparticles occur at the same boundary, leading to an increase (decrease) in the local density and the formation of incompressible QHSs with $\nu_{\mathrm{CF}} = 2$ ($\nu_{\mathrm{CF}} = 1$). If we rotate the current to the vertical direction (blue arrow), the incompressible regions rotate as well. In short, the current passing through the disordered 2DES induces incompressible phases at domain boundaries that are always parallel to the current direction. This explains why we measure the same κ in different current directions as shown in Fig. 3(e). Similar discussion can be easily extended to QHSs, where the flowing current drives the sparsely distributed, disorder-pinned quasiparticles and quasiholes out of their equilibrium positions and piles them at boundaries of the incompressible liquid phase.

In conclusion, we use the interaction between SAW and electrons to study the morphing of quantum phases in ultra-high-mobility 2DESs. We discover that the SAW velocity increases, suggesting that the 2DES becomes more

incompressible when a nondestructive current flows through the 2DES. This effect is only seen with a revolutionary enhanced sound velocity resolution at very low temperatures and disappears at $T \gtrsim 250$ mK.

We acknowledge support by the National Key Research and Development Program of China (Grants No. 2021YFA1401900 and No. 2019YFA0308403) and the National Natural Science Foundation of China (Grants No. 92065104 and No. 12074010) for sample fabrication and measurement. The Princeton University portion of this research is funded in part by the Gordon and Betty Moore Foundation's EPiQS Initiative, Grant No. GBMF9615.01 to L. P.. We thank Xin Wan, Zhao Liu, and Bo Yang for valuable discussions.

*Corresponding author: xilin@pku.edu.cn
†Corresponding author: liuyang02@pku.edu.cn

[1] D. C. Tsui, H. L. Stormer, and A. C. Gossard, Phys. Rev. Lett. **48**, 1559 (1982).
[2] R. E. Prange and S. M. Girvin, eds., *The Quantum Hall Effect* (Springer, New York, 1987).
[3] J. K. Jain, *Composite Fermions* (Cambridge University Press, Cambridge, England, 2007).
[4] M. P. Lilly, K. B. Cooper, J. P. Eisenstein, L. N. Pfeiffer, and K. W. West, Phys. Rev. Lett. **82**, 394 (1999).
[5] R. R. Du, D. C. Tsui, H. L. Stormer, L. N. Pfeiffer, K. W. Baldwin, and K. W. West, Solid State Commun. **109**, 389 (1999).
[6] A. A. Koulakov, M. M. Fogler, and B. I. Shklovskii, Phys. Rev. Lett. **76**, 499 (1996).
[7] R. L. Willett, J. P. Eisenstein, H. L. Störmer, D. C. Tsui, A. C. Gossard, and J. H. English, Phys. Rev. Lett. **59**, 1776 (1987).
[8] W. Pan, J.-S. Xia, V. Shvarts, D. E. Adams, H. L. Stormer, D. C. Tsui, L. N. Pfeiffer, K. W. Baldwin, and K. W. West, Phys. Rev. Lett. **83**, 3530 (1999).
[9] C. R. Dean, B. A. Piot, P. Hayden, S. Das Sarma, G. Gervais, L. N. Pfeiffer, and K. W. West, Phys. Rev. Lett. **101**, 186806 (2008).
[10] A. Kumar, G. A. Csáthy, M. J. Manfra, L. N. Pfeiffer, and K. W. West, Phys. Rev. Lett. **105**, 246808 (2010).
[11] E. H. Rezayi and F. D. M. Haldane, Phys. Rev. Lett. **84**, 4685 (2000).
[12] M. R. Peterson, T. Jolicoeur, and S. Das Sarma, Phys. Rev. Lett. **101**, 016807 (2008).
[13] A. Wójs, C. Tőke, and J. K. Jain, Phys. Rev. Lett. **105**, 096802 (2010).
[14] R. L. Willett, Rep. Prog. Phys. **76**, 076501 (2013).
[15] X. Lin, R. Du, and X. Xie, Natl. Sci. Rev. **1**, 564 (2014).
[16] X. Wan, Z.-X. Hu, E. H. Rezayi, and K. Yang, Phys. Rev. B **77**, 165316 (2008).
[17] G. Moore and N. Read, Nucl. Phys. **B360**, 362 (1991).
[18] A. Kitaev, Ann. Phys. (Amsterdam) **303**, 2 (2003).
[19] A. Stern, Nature (London) **464**, 187 (2010).
[20] C. Nayak, S. H. Simon, A. Stern, M. Freedman, and S. Das Sarma, Rev. Mod. Phys. **80**, 1083 (2008).
[21] S. Roddaro, V. Pellegrini, F. Beltram, G. Biasiol, L. Sorba, R. Raimondi, and G. Vignale, Phys. Rev. Lett. **90**, 046805 (2003).
[22] J. B. Miller, I. P. Radu, D. M. Zumbühl, E. M. Levenson-Falk, M. A. Kastner, C. M. Marcus, L. N. Pfeiffer, and K. W. West, Nat. Phys. **3**, 561 (2007).
[23] I. P. Radu, J. B. Miller, C. M. Marcus, M. A. Kastner, L. N. Pfeiffer, and K. W. West, Science **320**, 899 (2008).
[24] H. Fu, P. Wang, P. Shan, L. Xiong, L. N. Pfeiffer, K. West, M. A. Kastner, and X. Lin, Proc. Natl. Acad. Sci. U.S.A. **113**, 12386 (2016).
[25] R. L. Willett, L. N. Pfeiffer, and K. W. West, Proc. Natl. Acad. Sci. U.S.A. **106**, 8853 (2009).
[26] Y. Zhang, D. T. McClure, E. M. Levenson-Falk, C. M. Marcus, L. N. Pfeiffer, and K. W. West, Phys. Rev. B **79**, 241304(R) (2009).
[27] R. L. Willett, L. N. Pfeiffer, and K. W. West, Phys. Rev. B **82**, 205301 (2010).
[28] J. Nakamura, S. Liang, G. C. Gardner, and M. J. Manfra, Nat. Phys. **16**, 931 (2020).
[29] L. Saminadayar, D. C. Glattli, Y. Jin, and B. Etienne, Phys. Rev. Lett. **79**, 2526 (1997).
[30] R. de Picciotto, M. Reznikov, M. Heiblum, V. Umansky, G. Bunin, and D. Mahalu, Nature (London) **389**, 162 (1997).
[31] A. Bid, N. Ofek, H. Inoue, M. Heiblum, C. L. Kane, V. Umansky, and D. Mahalu, Nature (London) **466**, 585 (2010).
[32] M. Dolev, Y. Gross, Y. C. Chung, M. Heiblum, V. Umansky, and D. Mahalu, Phys. Rev. B **81**, 161303(R) (2010).
[33] W. E. Chickering, J. P. Eisenstein, L. N. Pfeiffer, and K. W. West, Phys. Rev. B **87**, 075302 (2013).
[34] M. Banerjee, M. Heiblum, A. Rosenblatt, Y. Oreg, D. E. Feldman, A. Stern, and V. Umansky, Nature (London) **545**, 75 (2017).
[35] M. Banerjee, M. Heiblum, V. Umansky, D. E. Feldman, Y. Oreg, and A. Stern, Nature (London) **559**, 205 (2018).
[36] A. Wixforth, J. P. Kotthaus, and G. Weimann, Phys. Rev. Lett. **56**, 2104 (1986).
[37] M. A. Paalanen, R. L. Willett, P. B. Littlewood, R. R. Ruel, K. W. West, L. N. Pfeiffer, and D. J. Bishop, Phys. Rev. B **45**, 11342 (1992).
[38] R. L. Willett, R. R. Ruel, K. W. West, and L. N. Pfeiffer, Phys. Rev. Lett. **71**, 3846 (1993).
[39] R. L. Willett, K. W. West, and L. N. Pfeiffer, Phys. Rev. Lett. **88**, 066801 (2002).
[40] B. Friess, V. Umansky, K. von Klitzing, and J. H. Smet, Phys. Rev. Lett. **120**, 137603 (2018).
[41] B. Friess, I. A. Dmitriev, V. Umansky, L. Pfeiffer, K. West, K. von Klitzing, and J. H. Smet, Phys. Rev. Lett. **124**, 117601 (2020).
[42] B. Friess, Y. Peng, B. Rosenow, F. von Oppen, V. Umansky, K. von Klitzing, and J. H. Smet, Nat. Phys. **13**, 1124 (2017).
[43] I. L. Drichko, I. Y. Smirnov, A. V. Suslov, and D. R. Leadley, Phys. Rev. B **83**, 235318 (2011).
[44] I. L. Drichko, I. Y. Smirnov, A. V. Suslov, Y. M. Galperin, L. N. Pfeiffer, and K. W. West, Phys. Rev. B **94**, 075420 (2016).
[45] Previous work in Ref. [36] explains the velocity shift with the conductivity. Such an analysis may not be suitable here

because our ultra-high-mobility 2DES has a very long transport scattering time $\tau_{tr} \simeq 0.7$ ns comparable to the SAW frequency.

[46] R. M. White and F. W. Voltmer, Appl. Phys. Lett. **7**, 314 (1965).

[47] M. Wu, X. Liu, R. Wang, X. Lin, and Y. Liu, arXiv:2311.01718.

[48] See Supplemental Material at http://link.aps.org/supplemental/10.1103/PhysRevLett.132.076501 for a detailed description of our setup, which includes Refs. [49,50].

[49] D. Sullivan, D. Allan, D. Howe, and F. Walls, NIST Technical Note 1337 (National Institute of Standards and Technology, 1990), https://nvlpubs.nist.gov/nistpubs/Legacy/TN/nbstechnicalnote1337.pdf#page=13.

[50] P. Durdaut, M. Höft, J.-M. Friedt, and E. Rubiola, Sensors **19**, 185 (2019).

[51] Y. P. Chen, R. M. Lewis, L. W. Engel, D. C. Tsui, P. D. Ye, L. N. Pfeiffer, and K. W. West, Phys. Rev. Lett. **91**, 016801 (2003).

[52] Such behavior is surprising but not inconsistent with the previous report, since our frequency is much lower than the geometric resonance condition [38,39].

[53] Y. J. Chung, K. W. Baldwin, K. W. West, N. Haug, J. van de Wetering, M. Shayegan, and L. N. Pfeiffer, Nano Lett. **19**, 1908 (2019).